Plant, Cell & Environment

Plant, Cell and Environment (2016) doi: 10.1111/pce.12774

Original Article

Most stomatal closure in woody species under moderate drought can be explained by stomatal responses to leaf turgor

Celia M. Rodriguez-Dominguez[1,2†], Thomas N. Buckley[3†], Gregorio Egea[4], Alfonso de Cires[2], Virginia Hernandez-Santana[1], Sebastia Martorell[5] & Antonio Diaz-Espejo[1]

[1]Irrigation and Crop Ecophysiology Group, Instituto de Recursos Naturales y Agrobiología de Sevilla (IRNAS, CSIC), Avenida Reina Mercedes 10, 41012 Seville, Spain, [2]Departamento de Biología Vegetal y Ecología, Universidad de Sevilla, Seville, Spain, [3]IA Watson Grains Research Centre, Plant Breeding Institute, Faculty of Agriculture and Environment, The University of Sydney, Narrabri, NSW 2390, Australia, [4]Área de Ingeniería Agroforestal, Escuela Técnica Superior de Ingeniería Agronómica, Universidad de Sevilla, Ctra Utrera, km 1, 41013 Seville, Spain and [5]Research Group on Plant Biology under Mediterranean Conditions, Departament de Biologia, Universitat de les Illes Balears, Carretera de Valldemossa Km 7.5, 07122 Palma, Illes Balears, Spain

ABSTRACT

Reduced stomatal conductance (g_s) during soil drought in angiosperms may result from effects of leaf turgor on stomata and/or factors that do not directly depend on leaf turgor, including root-derived abscisic acid (ABA) signals. To quantify the roles of leaf turgor-mediated and leaf turgor-independent mechanisms in g_s decline during drought, we measured drought responses of g_s and water relations in three woody species (almond, grapevine and olive) under a range of conditions designed to generate independent variation in leaf and root turgor, including diurnal variation in evaporative demand and changes in plant hydraulic conductance and leaf osmotic pressure. We then applied these data to a process-based g_s model and used a novel method to partition observed declines in g_s during drought into contributions from each parameter in the model. Soil drought reduced g_s by 63–84% across species, and the model reproduced these changes well ($r^2 = 0.91$, $P < 0.0001$, $n = 44$) despite having only a single fitted parameter. Our analysis concluded that responses mediated by leaf turgor could explain over 87% of the observed decline in g_s across species, adding to a growing body of evidence that challenges the root ABA-centric model of stomatal responses to drought.

Key-words: abscisic acid; isohydric; process-based model; stomata; stomatal limitation; transpiration; water stress.

INTRODUCTION

Stomata regulate the trade-off between carbon gain and water loss in leaves. Declines in stomatal conductance (g_s) during soil drought greatly impact crop production and ecosystem function across the globe (Hetherington & Woodward 2003), yet the mechanisms for this response remain poorly understood. In particular, it remains unresolved whether hydraulic or hormonal mechanisms are responsible. One hypothesis that has dominated popular perception for many years is that decline in g_s during drought is mostly driven by hormonal signals such as abscisic acid (ABA) that are generated independent of leaf water status (Davies & Zhang 1991; Tardieu & Simonneau 1998; Dodd 2005). An alternative hypothesis is that stomatal closure during soil drought is caused by an actively mediated negative feedback response of stomata to reduced leaf turgor (Sperry *et al.* 2002; Buckley 2005; Brodribb & Cochard 2009). The conflict between these two viewpoints has dominated discussion of stomatal regulation for years yet shows no sign of abating (Schachtman & Goodger 2008; Pantin *et al.* 2012; Brodribb & McAdam 2013; Dodd 2013; Franks 2013).

Strong, albeit circumstantial, support can be found for both viewpoints. The root-ABA hypothesis is supported by two lines of evidence: the fact that stomatal closure during drought can occur with little or no measurable decline in leaf water potential, ψ_{leaf}, that is, 'isohydric' behaviour (e.g. Bates & Hall 1981; Tardieu 1993), and the observation that dried roots produce ABA that ends up in the xylem sap, which provides a mechanism of regulation because ABA is well known to cause stomatal closure (Downtown *et al.* 1988; Tardieu & Davies 1992; Dodd *et al.* 2008). However, other evidence questions whether root-derived ABA signals are necessary to explain isohydric behaviour or stomatal closure in drought more generally. For example, modelling has shown that negative feedback from leaf turgor can produce a state of near homeostasis in ψ_{leaf} that may be experimentally indistinguishable from true homeostasis (Sperry 2000; Buckley 2005). Holbrook *et al.* (2002) observed normal stomatal responses to drought in tomato shoots grafted onto roots that cannot produce ABA and suggested that another chemical signal from drying roots may lead to changes in pH that cause release of leaf ABA stores. Other evidence implicates leaf-endogenous, rather than leaf-exogenous, ABA in stomatal responses to reduced water status: reductions in leaf turgor following an increase in evaporative demand can lead to ABA synthesis within leaves and subsequent decline in g_s (McAdam *et al.* 2016).

Despite the evidence that responses to leaf turgor may explain much, and possibly most g_s decline during drought, there remains a widespread perception among plant biologists that

Correspondence to: A. Diaz-Espejo. Fax: +34 954624711; E-mail: a.diaz@csic.es
†These authors contributed equally to this work.

stomata close during drought because of root-derived ABA signals (Li *et al.* 2011; Romero *et al.* 2012; Secchi *et al.* 2013). The persistence of this view led us to reconsider whether stomatal responses to leaf turgor are indeed capable of explaining observed drought responses quantitatively, or if instead leaf-exogenous ABA signals are required. Additionally, other factors may also contribute to changes in g_s during soil drought, including osmotic adjustment (Turner *et al.* 1978; Premachandra *et al.* 1992), changes in photosynthetic capacity (Mott 2009; Busch 2014; Lawson *et al.* 2014) and intercellular CO_2 concentration (Mott 1988), and subtle differences in environmental conditions between non-drought and drought conditions, such as reduced air humidity or increased temperature accompanying soil drying.

The objective of this study was to test the hypothesis that observed stomatal closure during soil drought requires a major contribution from leaf-exogenous ABA signals, given what we currently know about stomatal water relations, mechanics and responses to leaf turgor. A central challenge in separating the roles of leaf and root water status in driving stomatal behaviour during drought is the fact that a decline in soil water potential will directly reduce both leaf and root turgor by equal amounts. We therefore used a dataset that included not only a drought treatment but also wide and independent variation in leaf and root turgor generated by other factors, including diurnal variations in vapour pressure deficit, changes in plant hydraulic conductance and species differences in the degree of isohydry during drought. We then tested whether a model that includes both leaf turgor-dependent and leaf turgor-independent responses could explain this diverse dataset, and we used a novel partitioning approach (adapted from Buckley & Diaz-Espejo 2015) to quantify the contributions of each factor in the model to observed stomatal closure in drought. Our results demonstrate that a large majority of the observed decline in g_s during drought across these three species can be explained without the need for leaf-exogenous ABA signals.

MATERIAL AND METHODS

Overview

Here we present a brief overview of our experimental and analytical approach. We measured leaf physiology in well-watered (WW) and water-stressed (WS) conditions in three species (almond, olive and grapevine), including parameters needed to predict g_s from a simplified form of the stomatal model of Buckley *et al.* (2003) (hereafter the BMF model). This model is based on the hypothesis that guard cell osmotic pressure is actively regulated in proportion to leaf turgor – that is, the hydroactive feedback hypothesis (HFH) – and on established biophysical process laws for water transport and gas exchange. However, the model also accommodates direct suppression of guard cell osmotic pressure by ABA signals that are generated independent of leaf turgor. We quantitatively partitioned observed changes in g_s between WW and WS treatments into additive contributions from each term in the model, using the method of Buckley & Diaz-Espejo (2015). These contributions included turgor-mediated effects of soil water potential, leaf osmotic pressure and plant hydraulic conductance, a turgor-independent effect representing leaf-exogenous ABA signals, and, in some cases, effects of minor differences in light and temperature between treatments. We note that this analytical approach cannot discern empirically whether leaf-exogenous ABA signals were in fact involved in the observed changes in g_s; rather, it allowed us to determine whether, and to what extent, those changes could be explained by leaf turgor-mediated effects, or if instead a dominant role for leaf-exogenous ABA signals must be invoked.

The BMF model remains, to date, the only available model of stomatal function that can be used to assess relationships among different factors involved in stomatal regulation in the context of well-established biophysical relationships among those factors. All other models, while useful in certain contexts, either were structured with the intention of reproducing empirical aspects of stomatal function rather than representing the underlying processes (e.g. Ball *et al.*, 1987, and Jarvis, 1976, type models) or are partially process based but either contradict fundamental aspects of stomatal hydromechanics – for example, Dewar (1995, 2002), Tardieu & Davies (1993), Tardieu *et al.* (2015) and Huber *et al.* (2014) – or only account for effects of changes in evaporative demand, and not in water potential or hydraulic conductance upstream of the leaf (e.g. Peak & Mott 2011). By contrast, the HFH upon which the BMF model is based was recently validated by experiments demonstrating *in vivo* a molecular mechanism for negative feedback regulation of guard cell osmotic pressure by leaf turgor (McAdam *et al.* 2016). Thus, although the conclusions of this study are theory laden in the sense that their validity depends to some degree upon that of the BMF model, the core premises of that model are in fact supported by a massive body of evidence (Buckley 2005).

Experimental conditions

The experiments occurred in 2012. The almond experiment was conducted at an orchard near Seville, Spain (37°15′N, −5°48′W). In early 2011, 20 one-year-old almond seedlings [*Prunus dulcis* (Mill.) D. A. Webb cv. Guara] were transplanted to 50 L pots containing a soil (*Arenic Albaqualf*, USDA 2010) with 69.3% sand, 28.6% clay and 2.1% silt (Fernández *et al.* 2011). Pots were placed in two rows oriented north to south, with 1.5 m between rows and 1 m between plants. A slow-release fertilizer (5 g pot^{-1} of Floranid® Permanent, NPK 16 + 7 + 15 + 2 MgO, Compo, BASF, Ludwigshafen, Germany) was applied every 40 d. The olive experiment was carried out at the same site as almond in a hedgerow olive orchard with 6-year-old olive trees (*Olea europaea* L. cv. Arbequina) at a spacing of 4 × 1.5 m (1667 trees ha^{-1}). The soil in the orchard (*Arenic Albaqualf*, USDA 2010) had a sandy loam top layer of 0.6 m and a sandy clay layer downwards (Fernández *et al.* 2013). The grapevine experiment was conducted in the experimental field of the University of Balearic Islands, Spain (39°38′ N, 2°38′E) using 3-year-old plants (*Vitis vinifera* L. cv. Grenache) planted in rows (2.5 m between rows and 1 m between plants) in natural clay loam soil 1.5 m deep. In all species, measurement cycles occurred on the same day in each of two

treatments: WW plants and plants experiencing imposed soil drought (WS).

All experimental sites have Mediterranean climate: hot and dry from May to September and mild and wet for the rest of the year. For almond, air temperature (T_a) and relative humidity (RH) were recorded by probes (ZIM Plant Technology GmbH, Hennigsdorf, Germany) near the pots and used to estimate leaf–air H_2O mole fraction gradient (Δw) given saturation vapour pressure at leaf temperature (Buck 1981), the air vapour pressure at each moment and the atmospheric pressure. For olive and grapevine, Δw was estimated from measurements of T_a and RH made at meteorological stations located in the same field as the experimental trees.

Irrigation and soil water status

Drip irrigation was used for all species. Almond pots were irrigated with $1.5\,L\,pot^{-1}\,d^{-1}$ until July, and then with $10\,L\,pot^{-1}\,d^{-1}$ from late July through mid-August. In the WW treatment, almond pots were irrigated to keep volumetric soil water content (SWC) near field capacity, and in the WS treatment, they were gradually stressed by withholding irrigation such that SWC was lower than in WW by $69 \pm 3\%$ on the day of measurements (when stomatal conductance significantly differed from WW). For olive, WW trees were irrigated enough to replace daily crop water demand (ET_c, mm), and in the WS treatment, a regulated deficit irrigation (DI) strategy was applied aimed to supply a total of 30% ET_c. For grapevine, in the WW treatment, irrigation was adjusted to maintain pre-dawn leaf water potential between −0.3 and −0.4 MPa, whereas in the WS treatment, irrigation was withheld throughout the summer. Drought levels differentially imposed to the three species were not relevant because the main objective of the present study was to clarify the role of turgor-mediated and hormonal mechanisms in diverse stomatal responses to soil drought.

Plant water status and gas exchange

Leaf water potential (ψ_{leaf}) was measured with a Scholander-type pressure chamber (PMS Instrument Company, Albany, Oregon, USA). Measurements were made from pre-dawn to sunset every 1.5–2 h on sun-exposed, healthy, fully developed leaves of representative current-year branches. In almond pots, two leaves from three plants per treatment were sampled; in olive trees, three leaves from one tree per treatment; and in grapevine plants, four leaves from four plants. ψ_{leaf} at pre-dawn was used as an estimate of soil water potential (ψ_{soil}).

Instantaneous measurements of stomatal conductance to H_2O (g_s) were made at 1.5 to 3 h intervals from dawn to sunset using an open-flow gas exchange system with a 2×3 cm chamber (Li-6400, Li-Cor Inc., Lincoln, NE, USA). Chamber radiation and temperature were set to match ambient conditions, and measurements were completed within 1–2 min of enclosing the leaf in the chamber, to ensure measured g_s was indicative of the value prevailing prior to measurements. In almond pots, measurements were made on two leaves per plant (similar to leaves chosen for ψ_{leaf} measurements) and four plants per treatment, and CO_2 concentration was controlled at $390\,\mu mol\,mol^{-1}$ by a 6400-01 CO_2 injector (Li-Cor Inc.). In olive trees, measurements were made on four leaves per treatment from the same trees sampled in ψ_{leaf} measurements, and ambient CO_2 concentration was used. In grapevine, one leaf from each of five plants was used, and CO_2 concentration was controlled at $400\,\mu mol\,mol^{-1}$. In all cases, photosynthetic photon flux densities (PPFDs) were measured with the internal photosynthetically active radiation (PAR) sensor from the open chamber of the Li-6400.

On the experimental dates, almond leaves were sampled at midday for osmotic pressure (π) measurements. One mature, full expanded leaf per plant in four plants per treatment was cleaned, packed in aluminium foil and immediately frozen in liquid nitrogen. One 7 mm diameter disc per leaf was sampled between the midrib and margin with a cork borer, punctured 15–20 times with forceps to speed equilibration and immediately loaded in a C-52 thermocouple psychrometer chamber (Wescor Inc., Logan, UT, USA) connected to a datalogger (PSYPRO, Wescor Inc.). Equilibrium was reached in ~30 min. We used the same procedure to measure π in four olive leaves per treatment sampled at dawn. We corrected π using the regression model of Bartlett *et al.* (2012) to account for apoplastic dilution and wall solute enrichment. In grapevine, π was estimated from five pressure–volume (P–V) curves per treatment, made with a Scholander chamber and an analytical balance (Kern ABT320-4M; KERN & SOHN, Balingen, Germany, 10^{-4} g resolution) (Martorell *et al.* 2015). π was assumed equal to leaf water potential at turgor loss point ($\psi_{\pi TLP}$), which was identified as the inflection point of the $1/\psi_{leaf}$ versus relative water content (RWC) curve. The fitting method proposed by Sack *et al.* (2011) was used to fit these curves.

Leaf osmotic pressure can change diurnally, especially as a result of fluctuations in leaf RWC. We therefore corrected the π values measured as described earlier by applying *in situ* measurements of leaf water potential to P–V curves for each species. For each species and treatment, we fitted a second-order polynomial to the relationship between water potential and leaf RWC and then used a dilution formula to correct π as needed by assuming osmotic content (moles) was diurnally invariant: $\pi(t) = \pi^* \cdot RWC(\psi^*_{leaf})/RWC(\psi_{leaf}(t))$, where $\pi(t)$ is the corrected value of π at time t, π^* is the π measurement described earlier, ψ^*_{leaf} is the leaf water potential corresponding to the condition in which π was initially measured (midday for almond, pre-dawn for olive and the turgor loss point for grapevine) and $RWC(\psi_{leaf}(t))$ represents the empirical P–V curve relationship between RWC and ψ_{leaf}.

Photosynthetic response curves

Responses of net CO_2 assimilation rate (A) to intercellular CO_2 concentration (c_i) (A-versus-c_i curves) were determined between 0900 and 1300 h Greenwich Mean Time (GMT) over the experimental period. Each curve comprised 15 measurements, each made after at least 3 min at a different value of ambient CO_2 concentration (c_a). After steady-state photosynthesis was achieved at $400\,\mu mol\,mol^{-1}$, c_a was lowered in seven steps

to 50 μmol mol^{-1}, then returned to 400 μmol mol^{-1} and increased in seven steps to 1700 μmol mol^{-1}. In almond, seven curves per treatment were determined at ambient temperature and saturating PPFD (2000 μmol m^{-2} s^{-1}). In olive, three curves per treatment were performed at ambient temperature and PPFD = 1600 μmol m^{-2} s^{-1}, and in grapevine, four curves per treatment were performed at 30 °C and PPFD = 1500 μmol m^{-2} s^{-1}. Parameters of the photosynthesis model of Farquhar *et al.* (1980) [mesophyll conductance (g_m), maximum carboxylation rate ($V_{c,max}$) and potential electron transport rate (J)] were estimated for each curve using the method of Ethier & Livingston (2004), which uses non-linear least squares regression to fit the parameters [we found no evidence of triosephosphate utilization (TPU) limitation in our data]. RuBisCo kinetic parameters and the photorespiratory CO_2 compensation point (Γ_*) were taken from Bernacchi *et al.* (2002). In almond, $V_{c,max}$, J_{max} and g_m were normalized to 25 °C using published temperature responses (Egea *et al.* 2011). In olive, normalized values to 25 °C of $V_{c,max}$ and J_{max} were obtained after recalculation of the temperature response of these parameters reported by Diaz-Espejo *et al.* (2006), considering the g_m temperature response (Diaz-Espejo *et al.* 2007). In grapevine, $V_{c,max}$, J_{max} and g_m were corrected to 25 °C using temperature responses published by Buckley *et al.* (2014). Parameter values used in this study for responses of photosynthetic parameters to temperature are summarized in Table S1, and values of $V_{c,max}$, J_{max} and g_m at 25 °C are shown in Table S2 of the Supporting Information File S1. J is modelled as the lesser root of a quadratic expression, $\theta J^2 - (J_{max} + \varphi i) \cdot J + J_{max} \cdot \varphi i = 0$, where i is PPFD and θ and φ are dimensionless empirical parameters (the convexity parameter and initial slope of J versus i, respectively). θ and φ were estimated in almond and olive by fitting the model to A-versus-PPFD response curves (four curves per treatment in almond and three in olive) performed by reducing PPFD from 2500 μmol m^{-2} s^{-1} (for almond) or 2000 μmol m^{-2} s^{-1} (for olive) to darkness in 15 steps using a LED Light Source (Li-6400-02B, Li-Cor Inc.) connected to the Li-6400. Temperature and c_a were 28–32 °C and 390 μmol mol^{-1}, respectively. The resulting values were $\theta = 0.71$ and $\varphi = 0.2$ (for almond) and $\theta = 0.91$ and $\varphi = 0.323$ (for olive). For grapevine, we used values of $\theta = 0.90$ and $\varphi = 0.385$ (given by Buckley *et al.*, 2014, for plants in the same trials, used in a different experiment). We used the same values for θ, φ, Γ_* and RuBisCo kinetic parameters to model both WW and WS; most data show that moderate drought does not affect these features of photosynthetic metabolism (Flexas *et al.* 2004). Additional information about the photosynthetic model is given in the Appendix and in Supporting Information File S1.

Statistical analysis

We used analysis of variance in linear models to quantify effects of irrigation treatment on $V_{c,max}$, J_{max}, g_m, K, n, a, π and ψ_{soil} within each species using base R (R Core Team 2014), using logarithmic transformation to improve normality when needed. Midday averages were used for K and a.

Model of stomatal conductance based on the hydroactive feedback hypothesis

We used a modified form of the g_s model originally presented by Buckley *et al.* (2003) (the BMF model) to examine the mechanistic basis of observed changes in g_s, in order to assess whether those changes could be explained by the HFH or if instead they required a substantial contribution from leaf-exogenous ABA signals. This model is based on biophysical process descriptions for gas exchange, water relations and stomatal hydromechanics and on the HFH, which states that guard cell osmotic pressure is actively regulated in proportion to epidermal turgor pressure (which acts as a sensor for changes in leaf water status). In the BMF model, effects of light and intercellular CO_2 concentration on guard cell osmotic pressure are predicted using an empirical sub-model (Farquhar & Wong 1984). In the Supporting Information File S1, we present the model in greater detail, and we derive the following modified form of the model:

$$g_s = \frac{naK(\psi_{soil} + \pi)}{K + na\Delta w} \quad (1)$$

where K is leaf-specific hydraulic conductance, ψ_{soil} is soil water potential, π is bulk leaf osmotic pressure and Δw is leaf-to-air water vapour mole fraction gradient. The product na in Eqn 1 is equivalent to the product $\chi\beta\tau$ in the simplified BMF model, where β is the sensitivity of guard cell osmotic pressure to changes in leaf turgor, τ is a factor that captures the effects of light and CO_2 on guard cell osmotic pressure and χ is a proportionality factor that scales the mechanical effects of guard and epidermal cell turgor pressures on stomatal aperture to g_s units. Leaf turgor (P), which depends on transpiration rate and on g_s itself, is implicit in the parameters and variables of Eqn 1 ($P = \pi + \psi_{leaf} = \pi + \psi_{soil} - \Delta w \cdot g_s/K$).

This equation thus includes three categories of effectors of stomatal responses during drought: direct effects of changes in K, ψ_{soil} and π (which are mediated by changes in P), changes in PPFD and c_i (mediated by a) and changes in other factors that do not directly depend on P, PPFD or c_i (mediated by n). The term τ, which acts as a sensor for PPFD and c_i in the BMF model, originated in an earlier model by Farquhar & Wong (1984), who noted that stomatal responses to PPFD and c_i were remarkably similar to responses of mesophyll adenosine triphosphate (ATP) concentration (τ) to PPFD and c_i predicted by the photosynthesis model of Farquhar *et al.* 1980. We used the ATP model presented by Farquhar & Wong (1984) as an empirical model to capture the effects of PPFD and c_i on g_s. Because τ also scales with the total adenylate pool (τ_m), and thus with photosynthetic capacity (Farquhar & Wong 1984), we separated the effects of PPFD and c_i from that of photosynthetic capacity by incorporating τ_m into the parameter n. Thus, the parameters n and a both capture turgor-independent or 'non-hydraulic' effects – a is τ expressed relative to its maximum value and n is a lumped parameter representing other turgor-independent factors – and are defined in terms of the BMF and Farquhar–Wong model parameters as follows:

$$n \equiv \chi\beta\tau_m \quad (2)$$

$$a \equiv \tau/\tau_m \quad (3)$$

There is a mechanistic basis for using the term n in Eqn 1 to capture effects of leaf-exogenous ABA. Buckley *et al.* (2003) showed, following Dewar (2002), that the parameter β can be interpreted as the ratio of the specific rates of active ion uptake and passive ion efflux in guard cells; thus, because ABA affects guard cells by stimulating passive efflux of osmotic solutes (Hetherington 2001), drought-induced increases in ABA should cause β, and thus n, to decline (see the Supporting Information File S1 for a derivation of this relationship).

How we applied the model

To apply the modified BMF model (Eqn 1), we simulated a using the model of Farquhar & Wong (1984), we estimated K as $g_s \cdot \Delta w/(\psi_{soil} - \psi_{leaf})$, and we measured π, ψ_{soil} and Δw as described earlier. Finally, we estimated the parameter n by fitting Eqn 1 to six to eight diurnal measurements of g_s in each leaf for four to five different leaves, using Solver in Microsoft Excel to minimize the sum of squared differences between modelled and measured g_s. We assumed the parameters n and ψ_s were diurnally invariant, and we used values of π corrected as described earlier for diurnal changes in leaf water content. Note that goodness-of-fit measures estimated for the model fitted in this way are likely inflated, because K is computed using measured g_s and then used to model g_s. However, we were not testing the model as a stand-alone predictive tool but rather using it as a tool for explanation and interpretation, so the autocorrelation between measured and modelled g_s introduced by using K in this manner does not affect interpretation of our results.

Partitioning changes in g_s into contributions from different variables

We used the method of Buckley & Diaz-Espejo (2015) to partition changes in g_s into contributions from the underlying variables. This method was originally designed to partition changes in net CO_2 assimilation rate (A) into contributions from variables in the photosynthesis model of Farquhar *et al.* (1980) by numerically integrating the exact differential of A (dA) across the interval over which A changed. The exact differential of a function parses an infinitesimal change in the function into contributions from each variable. Applied to g_s in Eqn 1, this gives

$$dg_s = \frac{\partial g_s}{\partial n}dn + \frac{\partial g_s}{\partial a}da + \frac{\partial g_s}{\partial K}dK + \frac{\partial g_s}{\partial \psi_{soil}}d\psi_{soil} + \frac{\partial g_s}{\partial \pi}d\pi \quad (4)$$

Numerically integrating Eqn 4 between a WW point and a drought (WS) point gives finite *partial changes* in g_s due to each variable, which add up to the total change in g_s:

$$\int_{WW}^{WS} dg_s = \int_{WW}^{WS} \left(\frac{\partial g_s}{\partial n}dn + \frac{\partial g_s}{\partial a}da + \frac{\partial g_s}{\partial K}dK + \frac{\partial g_s}{\partial \psi_{soil}}d\psi_{soil} + \frac{\partial g_s}{\partial \pi}d\pi \right) \quad (5a)$$

$$g_{s,WS} - g_{s,WW} = \sum_j \left(\int_{WW}^{WS} \frac{\partial g_s}{\partial x_j}dx_j \right) = \sum_j p_j \quad (5b)$$

where x_j denotes n, a, K, ψ_{soil} or π and p_j is the partial change in g_s due to x_j. Each variable's *contribution* (denoted C_j) to the total change in g_s is then computed by expressing its partial change as a percentage of the WW value of g_s (Eqn 6):

$$C_j = \frac{100}{g_{s,WW}}p_j \quad (6)$$

Note that the contribution for a variable is a negative number if its effect on g_s is negative; thus, for example, if g_s declined by 50% in drought and half of this decline was due to direct effects of ψ_{soil}, then C for ψ_{soil} would be –25%. Additional details describing the partitioning method and its implementation are given in the Appendix and in Supporting Information File S1.

RESULTS

Soil water potential, ψ_{soil}, estimated as pre-dawn leaf water potential, was lower in the WS treatment than in the WW treatment by 1.09, 1.22 and 0.61 MPa in almond, olive and grapevine, respectively (Fig. 1). However, despite the large decline in ψ_{soil} in almond, its midday leaf water potential (averaged between 1100 and 1400 h GMT) was only 0.18 MPa lower in WS than in WW; by contrast, midday ψ_{leaf} was 2.31 MPa lower in WS in olive and 0.88 MPa lower in grapevine. These declines in ψ_{leaf} were accompanied by reductions in midday stomatal conductance, g_s, of 63% in almond, 84% in olive and 83% in grapevine (Fig. 2), in WS relative to WW, and resulted in concurrent declines in leaf turgor and g_s (Figure S2 of Supporting Information File S1).

Model fitting

We fitted the BMF model to our data and then partitioned the observed declines in g_s into contributions from each variable in the model. Despite having only one fitted parameter (n, the turgor-independent or non-hydraulic parameter), the model was able to reproduce observed patterns of g_s (Figs 2 and 3). Modelled and measured g_s were linearly related with a slope of 1.05 and $r^2 = 0.91$ (Fig. 3). Residuals were uncorrelated with Δw and ψ_{soil} ($P > 0.05$) and weakly correlated with PPFD ($r^2 = 0.18$; $P < 0.001$; not shown) because of a tendency of the model to underestimate g_s at very low PPFD ($<200\,\mu mol\,m^{-2}\,s^{-1}$); however, residuals were uncorrelated with PPFD at midday irradiances, which were the focus of this analysis. When K was also included as a fitted parameter in the model, in addition to n, the model still simulated measured g_s satisfactorily, and fitted and measured midday averages of K agreed well (slope 0.87, $r^2 = 0.69$, $P < 0.0001$, Figure S3 of Supporting Information File S1).

Differences in model parameters between WW and WS varied among species (Fig. 4). Midday average K declined by 29, 91 and 88% in almond, olive and grapevine, respectively. The turgor-independent parameter n declined by 30, 0.3 and 62% in almond, olive and grapevine, respectively. Relative ATP concentration (a) increased during drought in all species, as expected given the reduction in c_i caused by partial stomatal closure, but whereas this increase was small in almond and

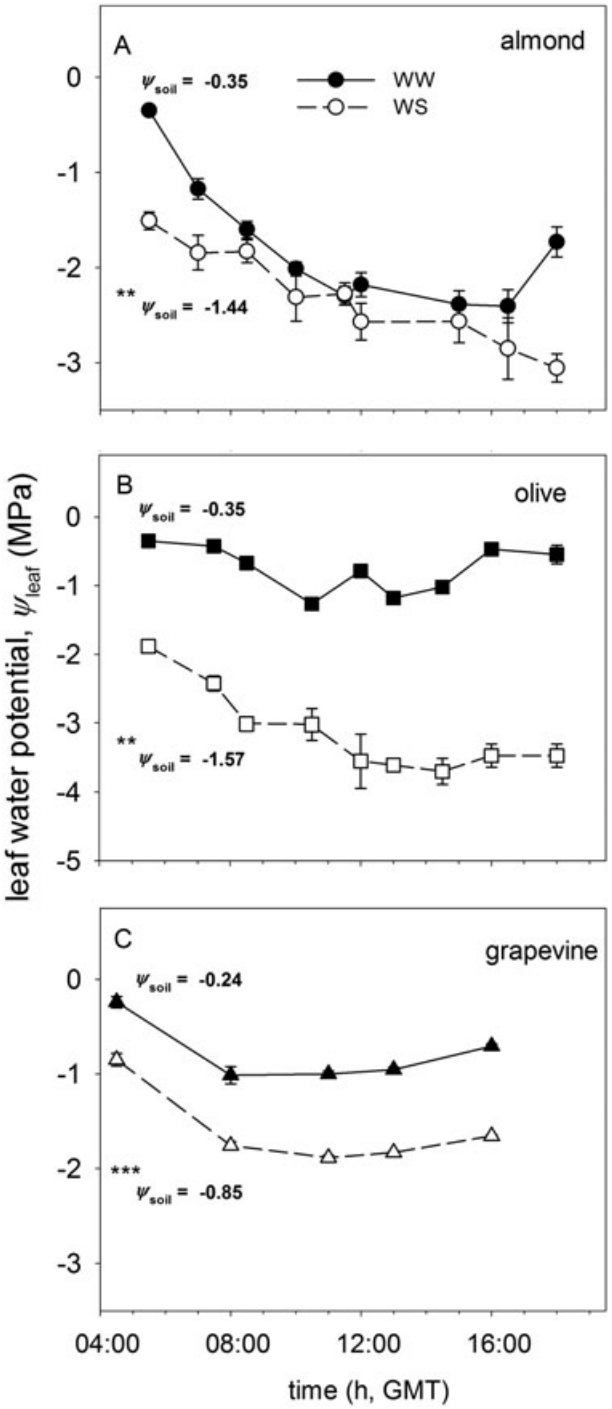

Figure 1. Diurnal courses of leaf water potential (ψ_{leaf}) in (a) almond (circles), (b) olive (squares) and (c) grapevine (triangles) in well-watered (WW: solid symbols and lines) and water-stressed (WS: open symbols and dashed lines) plants. Bars are standard errors, $n = 3$ (almond and olive) and $n = 4$ (grapevine). Soil water potentials (ψ_{soil}) are shown for each species, being the upper for WW and the lower for WS. GMT = Greenwich Mean Time. Asterisks denote significant treatment effects in ψ_{soil} within species: **, $P < 0.01$; ***, $P < 0.001$.

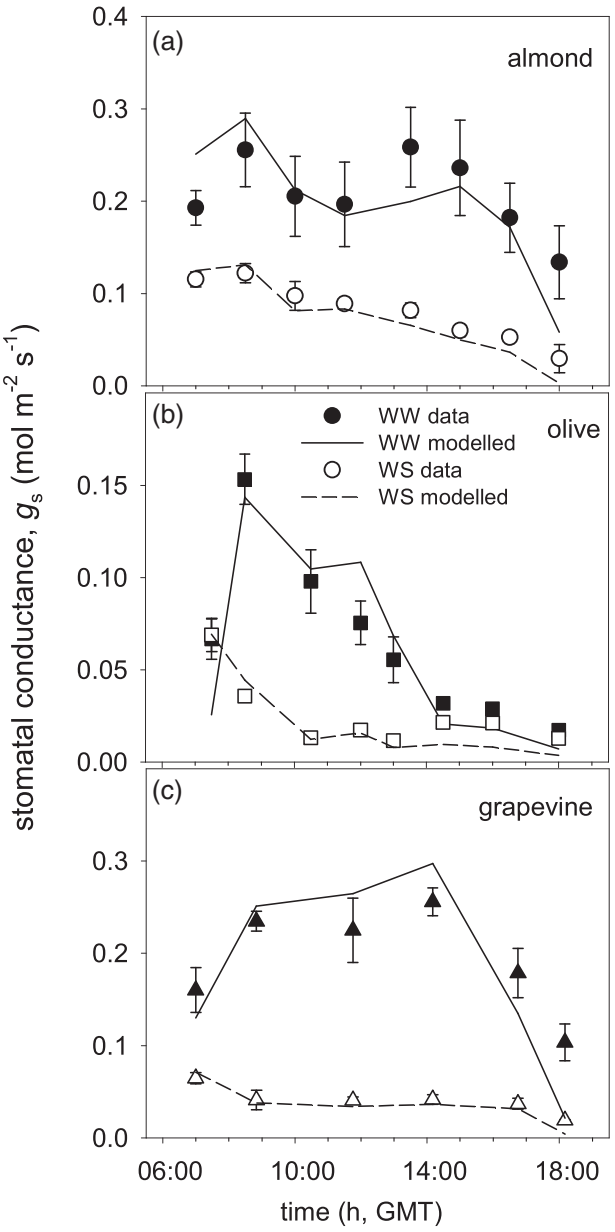

Figure 2. Diurnal trends in measured (symbols) and modelled (lines) stomatal conductance, g_s, in (a) almond, (b) olive and (c) grapevine under well-watered (WW, closed symbols and solid lines) and water-stressed (WS, open symbols and dashed lines) conditions. Bars are standard errors for measured g_s, $n = 4$ (almond and olive) and $n = 5$ (grapevine). GMT = Greenwich Mean Time. Symbols same as for Figure 1.

grapevine (16 and 20%, respectively), it was quite large in olive (86%). However, this was due to the fact that midday PPFD was greater in WS than WW in olive, whereas PPFD was similar in WS and WW in the other species. Midday average bulk leaf osmotic pressure, π, increased by 55% in olive and 14% in grapevine but decreased 9% in almond.

Contributions of each parameter to observed declines in g_s

The contributions of each variable to the observed changes in g_s (averaged across the midday period, from

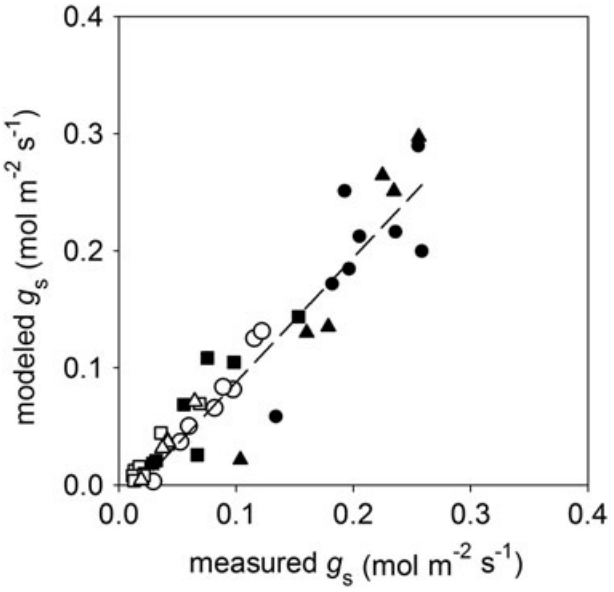

Figure 3. Relationship between measured and modelled values of stomatal conductance, g_s (slope = 1.05, $r^2 = 0.91$, $P < 0.0001$, $n = 44$; data for all species and both treatments combined). Symbols same as for Figure 1.

1100 to 1400 h) differed across species (Fig. 5). For example, sharp declines in hydraulic conductance (K) in both olive and grapevine contributed 88 and 60% declines in g_s, respectively, but in almond, K contributed only an 11% decline in g_s. The direct effect of soil water potential on g_s via reduced leaf turgor contributed a 40% decline in g_s in almond, versus 50 and 27% declines in olive and grapevine, respectively. Together, the observed changes in these two turgor-mediated variables contributed declines in g_s of 51% in almond, 138% in olive and 87% in grapevine – in each case explaining most of the total observed decline in g_s (negative contributions exceeding 100% are possible because the contributions from some other factors were positive, such that the total decline in g_s was below 100%). These contributions were further modified by osmotic adjustment, and particularly in olive, in which increases in π under water stress contributed a 44% increase in g_s (cross-hatched and green bars in Fig. 5). Osmotic adjustment had much smaller effects on g_s in almond and grapevine, contributing a 10% increase in g_s in both species.

Turgor-independent variables contributed much less than ψ_{soil} and K to the observed changes in g_s. The parameter n, which we expected to decrease in response to leaf-exogenous ABA signals, contributed declines of only 7 and 14% in g_s in almond and grapevine, respectively, and a negligible decline in olive (red bars in Fig. 5). The parameter a, which captures stomatal responses to light and CO_2, contributed a very small increase in g_s in all species (+3 to +6%), due to the effect on g_s of the small decline in c_i that resulted from stomatal closure and, in olive, greater PPFD during the WS treatment than during the WW treatment.

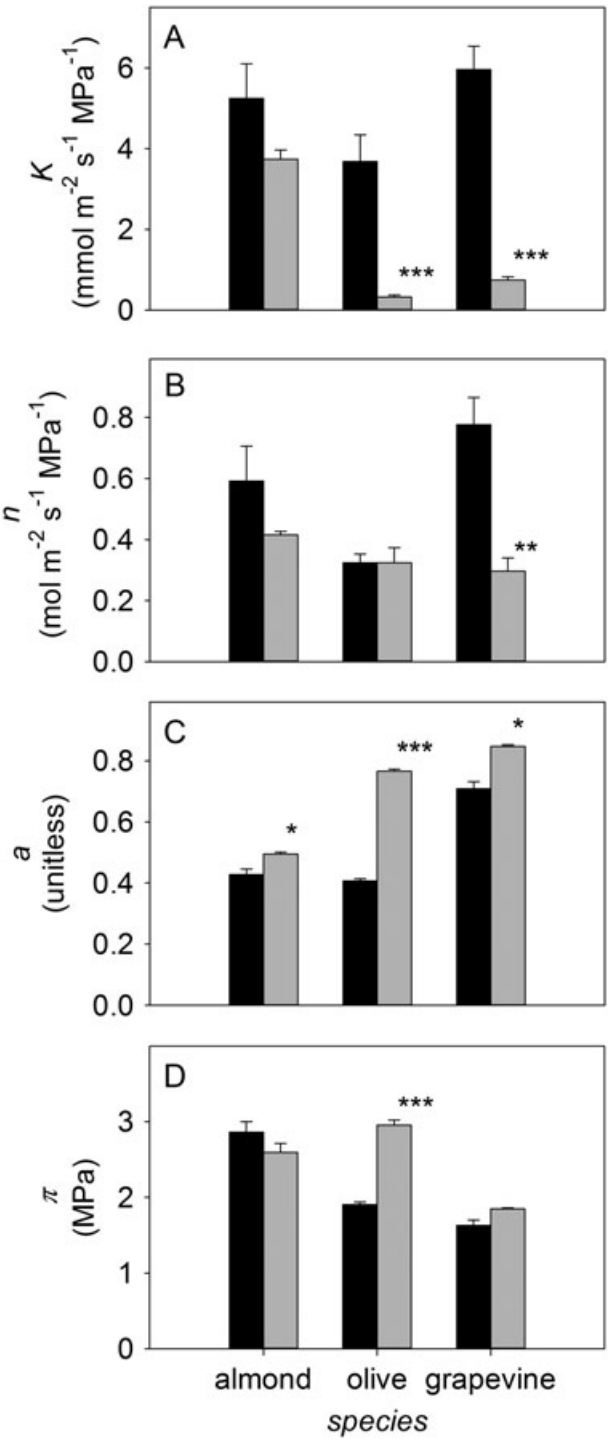

Figure 4. Differences in variables in the stomatal conductance model, between well-watered (WW) and water-stressed (WS) plants. (a) Soil-to-leaf hydraulic conductance, K. (b) The turgor-independent parameter, n, representing effects of hormonal signals on the sensitivity of guard cell osmotic pressure to leaf turgor. (c) Relative adenosine triphosphate (ATP) concentration, a. (d) Leaf osmotic pressure, π. The parameters K and π were measured, n was fitted and a was simulated with a photosynthesis model driven by measured photosynthetic and environmental parameters. Values shown for K and a are midday averages [between 1100 and 1400 h Greenwich Mean Time (GMT)]. Bars are standard errors; $n = 4$ (almond and olive) and $n = 5$ (grapevine). Asterisks denote significant treatment effects within species: *, $P < 0.05$; **, $P < 0.01$; ***, $P < 0.001$.

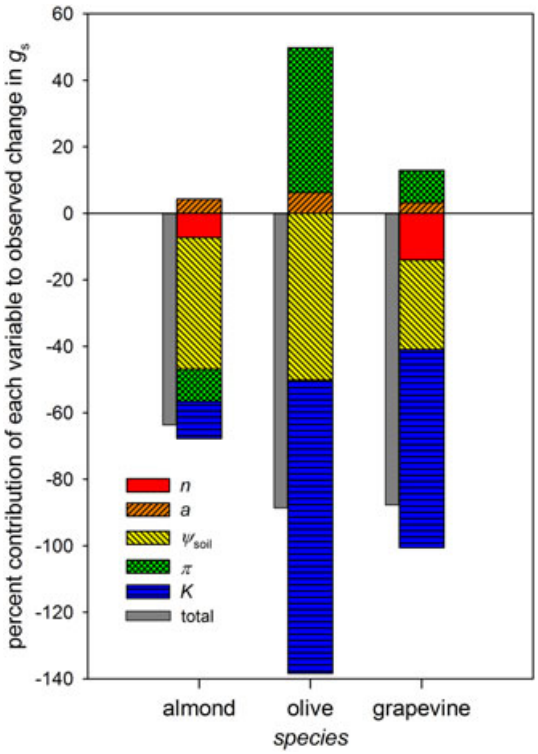

Figure 5. Percent contributions of different variables to the observed declines in midday stomatal conductance, g_s [averages from 1100 to 1400 h Greenwich Mean Time (GMT)], during soil drought. *n* is the turgor-independent parameter representing effects of hormonal signals on the sensitivity of guard cell osmotic pressure to leaf turgor; *a* is relative adenosine triphosphate (ATP) concentration, which captures stomatal responses to intercellular CO_2 (c_i) and photosynthetic photon flux density (PPFD); π is leaf osmotic pressure; ψ_{soil} is soil water potential; and *K* is plant hydraulic conductance. The total percent decline in g_s for each species is shown in narrow grey bars for reference.

Even when the positive contributions from osmotic adjustment were included together with those of *K* and ψ_{soil} in 'turgor-mediated effects', that category still explained most of the observed decline in g_s in each species, whereas turgor-independent effects of *n* and *a* contributed much less (cf. white and hatched bars in Fig. 6).

DISCUSSION

Both hydraulic and non-hydraulic factors have previously been proposed to explain stomatal closure during soil drought, but there is no consensus about which is more important (Tardieu & Simonneau 1998; Christmann *et al.* 2007). In particular, the role of root-derived ABA signals in driving stomatal closure during soil drought remains highly contentious (Bauer *et al.* 2013; Manzi *et al.* 2015; Munemasa *et al.* 2015; McAdam *et al.* 2016). We tested whether responses of stomatal guard cells to leaf turgor itself, as assumed by the HFH, could explain stomatal closure in soil drought, or if instead leaf turgor-independent mechanisms were required to enhance stomatal closure. We chose the terms 'turgor-mediated' and 'turgor-independent' effects, which are narrower than 'hydraulic' and 'non-hydraulic', in order to define more clearly the hypothesized role of leaf turgor and also to accommodate the influence of osmotic pressure (π) on turgor, given that π might not typically be considered a 'hydraulic' variable. We found that a simplified g_s model based on the HFH, having only a single fitted parameter and driven by physiological and environmental measurements, was able to reproduce stomatal behaviour very well ($r^2 = 0.91$) during drought across a dataset that included wide variation in factors that influence leaf and root turgor differently (e.g. changes in plant hydraulic conductance and leaf osmotic pressure), as required to separate their effects on stomatal control during drought. Our analysis showed that a single mechanism – a direct stomatal response to leaf turgor – could explain not only the changes in stomatal conductance resulting from diurnal variation in evaporative demand and changes in plant hydraulic conductance and osmotic pressure between treatments, but also the great majority (over 87% across species, and 100% in olive) of g_s decline during soil drought in three important woody crop species with differing resistance to drought, including deciduous (almond) and evergreen tree species (olive) and a temperate-deciduous liana species (grapevine). In order to reconcile these results with a root-ABA-centric model of stomatal responses to drought, one would have to assume that the response to leaf turgor becomes less sensitive during soil

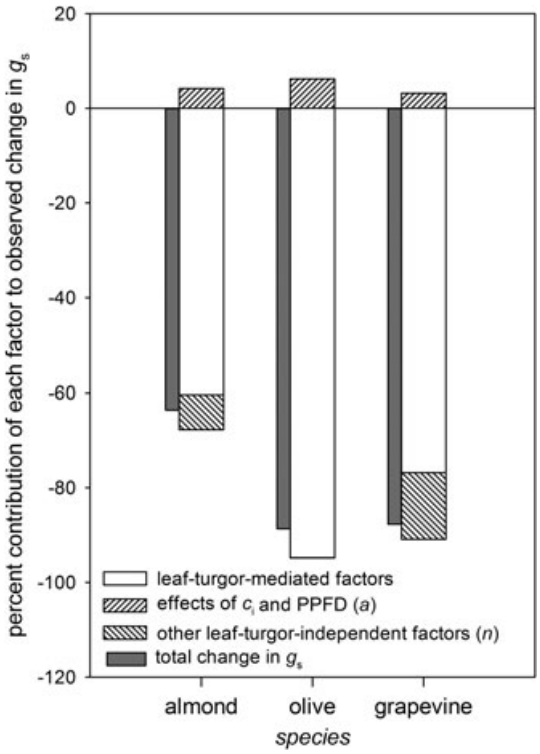

Figure 6. Percent contributions of leaf turgor-mediated and leaf turgor-independent factors that influence the observed declines in midday stomatal conductance, g_s [(averages from 1100 to 1400 h Greenwich Mean Time (GMT)], during soil drought in three species. Leaf turgor-mediated factors are the sum of *K*, ψ_{soil} and π as they are shown for each species in Fig. 5, and *n* and *a* are the same as in Fig. 5. The total percent decline in g_s for each species is shown with narrow grey bars for reference.

drought, to precisely the degree needed to make an independent root signal appear mathematically indistinguishable from the leaf turgor response. That assumption is highly unparsimonious, particularly in light of evidence that the leaf turgor response is itself mediated by leaf-endogenous ABA (McAdam *et al.* 2016): it would require leaves to be able to detect whether an ABA molecule came from roots, and if so, to suppress leaf ABA production or sensitivity accordingly.

Our conclusion does not imply that root signals do not occur; rather, it is evidence that they are quantitatively unimportant in stomatal responses to drought in these species, provided stomata respond to leaf turgor. This is consistent with a recent modelling study by Huber *et al.* (2014), in which root water uptake and transport during partial root zone drying (PRD) was simulated using a spatially explicit model coupled to an empirical model of stomatal conductance that included effects of leaf water status and root-derived ABA signals. Those authors found that effects of spatial and temporal heterogeneity in soil moisture within the root zone could 'largely be explained by hydraulic signalling'.

Which turgor-mediated factors drive g_s decline?

Our analysis suggested that a range of turgor-mediated factors, including hydraulic conductance (K), osmotic pressure (π) and soil water potential itself (ψ_{soil}), were responsible in varying degrees across our study species. For example, K declined sharply while π increased sharply in olive, whereas neither K nor π changed substantially in almond. As a result, although ψ_{leaf} declined far more in olive than in almond (by 1.67 versus 0.19 MPa), turgor dropped by similar amounts in both species (0.58 versus 0.41 MPa). These observed changes in K agree very well with each species' resistance to cavitation: almond is the most resistant, with an air entry point of −4.86 MPa (Cochard *et al.* 2008), in contrast to −1.55 MPa for olive (Diaz-Espejo *et al.* 2012) and −1.05 MPa for grapevine (Choat *et al.* 2010). Thus, differences in the coordination of hydraulic decline and osmotic adjustment may help to explain what makes some species anisohydric (e.g. olive) and others isohydric (e.g. almond).

Clarifying the potential roles of abscisic acid

Our results complement a growing body of evidence that questions the long-standing dogma (Dodd 2005; Goodger & Schachtman 2010; Torres-Ruiz *et al.* 2015) that stomatal closure in drought results primarily from leaf-exogenous ABA signals generated in drying roots (Davies & Zhang 1991; Tardieu & Davies 1993), and they complement a range of evidence that responses to leaf turgor may be equally or more important (Fuchs & Livingston 1996; Comstock and Mencuccini 1998; Yao *et al.* 2001). The hypothesis that root-derived ABA regulates g_s during soil drought has been extensively studied and has even impacted agriculture, through irrigation strategies based on PRD (Dodd *et al.* 2008). However, the importance of such signals is challenged by evidence that PRD is no more effective than DI (Sadras 2009; Egea *et al.* 2010). For example, Sadras (2009) analysed results from 15 field experiments comparing PRD with DI and found that the benefit of PRD was statistically indistinguishable from that of DI; he also found that g_s was minimally suppressed by PRD. Although one study found greater water use efficiency in PRD than DI, root-derived ABA signals were not involved in that case (Perez-Perez *et al.* 2012). This contrasts with results of Dodd (2009), who found a benefit of PRD over DI in six of 15 studies, although only one of those six was in a woody species (*V. vinifera* cv. Tempranillo) and it was performed in pots, which can suffer from artefacts (Passioura 2006). The role of long-distance chemical signalling in stomatal regulation has also been questioned in tall trees (Perks *et al.* 2002) and in experiments in which shoots were grafted onto rootstock deficient in ABA synthesis (Holbrook *et al.* 2002; Christmann *et al.* 2005). More recently, it has been suggested that ABA accumulation in WS roots depends on other sources (e.g. aerial organs) rather than on *de novo* synthesis in the roots (Waadt *et al.* 2014; Manzi *et al.* 2015).

The hydroactive feedback hypothesis

Our analysis demonstrated that leaf-exogenous ABA signals are not required to explain the majority of g_s decline during drought in our study species, provided that stomata respond directly to leaf turgor – that is, provided the HFH is valid. Thus, our conclusions could be challenged on the grounds that they are theory laden. This is true in principle, but the theory in question is grounded in a very large and growing body of experimental evidence. The HFH arose from the need to reconcile the fact that stomata eventually close when leaf water status decreases (e.g. Mott & Parkhurst 1991; Monteith 1995) with the fact that the direct, passive, mechanical effect of reduced leaf turgor in angiosperms is to open stomata, owing to the mechanical advantage of the epidermis (e.g. Franks *et al.* 2001; Franks & Farquhar 2007). One resolution to this paradox is to postulate that the mechanical advantage is overcome by an active stomatal response to leaf turgor (Darwin 1898; Meidner 1986). This hypothesis correctly predicts many distinctive features of stomatal behaviour, including (1) reversible short-term responses to changes in water potential elsewhere in the plant (Rufelt 1963; Raschke 1970; Fuchs & Livingston 1996; Whitehead *et al.* 1996; Comstock & Mencuccini 1998; Buckley & Mott 2000), (2) the transient opening that precedes stomatal closure in response to perturbations of leaf water status (Darwin 1898; Iwanoff 1928; Cochard *et al.* 2002), (3) the similarity in kinetics of responses to leaf water status and light (Grantz & Zeiger 1986), (4) stomatal aperture responses that match measured changes in epidermal turgor pressure (Mott & Franks 2001) and (5) the fact that leaf osmotic adjustment helps preserve g_s in drought (e.g. Turner *et al.* 1978; Hinckley *et al.* 1980; Premachandra *et al.* 1992; Shangguan *et al.* 1999). No other theory advanced to explain stomatal responses that involve water relations can claim so broad a foundation of empirical support. Nevertheless, the HFH has long remained speculative because the mechanism for hydroactive feedback was unknown. The recent discovery by McAdam *et al.* (2016) of leaf turgor-driven ABA synthesis has filled that gap by providing a demonstrated molecular mechanism for hydroactive feedback. Thus, although

our conclusions do assume the existence of hydroactive feedback responses of stomata to leaf turgor, that assumption is extremely well substantiated.

CONCLUSION

We found that most of the observed suppression of stomatal conductance during soil drought in almond, olive and grapevine could be attributed to direct responses of stomata to changes in leaf turgor (caused by changes in either soil water potential, hydraulic conductance or osmotic pressure) and that signals independent of leaf turgor were not required to explain most of the observed stomatal closure. These results support the HFH and add to the rapidly changing understanding of the potential role of hormonal signals in regulating gas exchange *in vivo*.

ACKNOWLEDGEMENTS

This work was funded by the Spanish Ministry of Science and innovation (research projects AGL2009-11310/AGR and AGL2012-34544/AGR) and co-funded by the FEDER programme. T. N. B. was supported by the National Science Foundation (award # 1146514) and the Australian Research Council (DP150103863 and LP130101183). C. M. R-D. benefited from an FPDI research fellowship from the Junta de Andalucía. We are grateful to A. Montero and A. Perez-Martin for assistance in the field.

Appendix Appendix: Equations used in the model analysis

This appendix presents equations necessary to reproduce the model-based partitioning analysis used in this study. Additional derivations and background are given in Supporting Information File S1.

i *Stomatal conductance model.* The reduced BMF model of g_s is

$$g_s = \frac{naK(\psi_{soil} + \pi)}{K + na\Delta w} \tag{A1}$$

where K is the whole-plant hydraulic conductance, ψ_{soil} is the soil water potential, π is the leaf osmotic pressure, Δw is the leaf-to-air water vapour mole fraction difference, a is the relative photosynthetic ATP concentration and n is a parameter representing effects of turgor-independent signals. In this study, K, ψ_{soil}, π and Δw were measured experimentally, a was simulated and n was fitted. The quantity a in Eqn A1 was simulated using the model of Farquhar & Wong (1984), which is based on the photosynthesis model of Farquhar *et al.* (1980). Different values of a apply under carboxylation-limited conditions (denoted with a subscript 'c') and regeneration-limited conditions (denoted with a subscript 'j'). That model can be written as

$$a_c = 1 - p' W_c / W_j \text{ and} \tag{A2}$$

$$a_j = (1 - p')(v - 1)/(vW_c/W_j - 1) \tag{A3}$$

where a_c and a_j are the values of a that apply under ribulose-1,5-bisphosphate (RuBP) carboxylation-limited and regeneration-limited conditions, respectively; W_c and W_j are the RuBP-saturated carboxylation rate and the carboxylation rate that can be sustained by the current rate of electron transport, respectively (defined in the following); p' is the ratio of the concentration of phosphorylation sites to the total adenylate concentration; and v is the ratio of the potential RuBP concentration (if all Calvin cycle carbon were in RuBP) to the total concentration of RuBisCo active sites (P' was taken as 0.2 and v as 2.27, following Buckley *et al.*, 2003). The actual value of a is then either a_c or a_j, depending on whether photosynthesis is limited by RuBP carboxylation or regeneration, respectively:

$$a = \begin{cases} a_c \\ a_j \end{cases} \text{ if } \begin{matrix} W_c < W_j \\ \text{else} \end{matrix} \tag{A4}$$

The carboxylation rates W_c and W_j (μmol m^{-2} s^{-1}) are given by

$$W_c = \frac{V_{c,max} c_c}{c_c + K_c(1 + O/K_o)} \text{ and} \tag{A5}$$

$$W_j = \frac{1}{4}\frac{J \cdot c_c}{c_c + \Gamma_*} \tag{A6}$$

where c_c is the chloroplastic CO_2 partial pressure [defined as $c_i - A/g_m$, where g_m is the mesophyll conductance to CO_2 (mol m^{-2} s^{-1}), c_i is the intercellular CO_2 concentration (μmol mol^{-1}) and A is the net CO_2 assimilation rate (μmol m^{-2} s^{-1}), calculated from the Farquhar model], $V_{c,max}$ is the maximum carboxylation rate (μmol m^{-2} s^{-1}), J is the potential electron transport rate (μmol m^{-2} s^{-1}), K_c and K_o are the Michaelis constants for RuBP carboxylation and oxygenation, respectively (both μmol mol^{-1}) and Γ_* is the photorespiratory CO_2 compensation point (μmol mol^{-1}). J is modelled as the lesser root of a quadratic expression, $\theta J^2 - (J_{max} + \varphi i) \cdot J + J_{max} \cdot \varphi i = 0$, where i is PPFD (μmol m^{-2} s^{-1}) and θ and φ are dimensionless empirical parameters (the convexity parameter and initial slope of J versus i, respectively). Several parameters in this photosynthesis model have a high dependence on temperature. We used the following equations to describe these temperature dependencies:

$$y(T_k) = y_{25} \exp(c_1 - c_3 T_k^{-1}) \left(\frac{1 + \exp(c_2 - c_4 T_r^{-1})}{1 + \exp(c_2 - c_4 T_k^{-1})} \right) \tag{A7}$$

$$y(T_k) = y_{25} \frac{\exp(c_1 - c_3 T_k^{-1})}{1 + \exp(c_2 - c_4 T_k^{-1})} \tag{A8}$$

$$y(T_k) = y_{25} \cdot \exp\left(-c_1 (\ln((T_k - 273.15)/c_2))^2 \right) \text{ and} \tag{A9}$$

$$y(T_k) = y_{25} \cdot c_1^{(T_k - T_r)/10} \tag{A10}$$

where $y(T_k)$ is the value of a parameter at a temperature T_k (Kelvin); y_{25} is the parameter's value at $T_k = 298.15$ K (25 °C); $T_r = 298.15$ K; and c_1, c_2, c_3 and c_4 are empirical parameters that vary among species and photosynthetic parameters. Different equations were used for different parameters in each species as suitable; Table S1 in Supporting Information File S1 lists values and sources for the parameter values used in this study.

ii *Partitioning changes in g_s into contributions from different factors.* Buckley & Diaz-Espejo (2015) presented a method for partitioning finite changes in CO_2 assimilation rate between

two measurement conditions into contributions from the underlying variables. We modified this method to partition changes in stomatal conductance, g_s, between WW and WS conditions. Here we present only the critical equations needed to apply the approach; additional detail is given in Supporting Information File S1. A change in g_s between WW and WS conditions is the sum of partial changes, p_j, due to each of the underlying variables x_j (where x_j is n, a, K, ψ_{soil}, π or Δw), where each partial change is the integral of the partial derivative of g_s with respect to x_j over the change in x_j:

$$g_{s,WS} - g_{s,WW} = \sum_j \left(\int_{WW}^{WS} \frac{\partial g_s}{\partial x_j} dx_j \right) = \sum_j p_j \quad \text{(A11)}$$

Our method estimates these integrals numerically as

$$p_j \approx \sum_{k=0}^{n-1} \left(g_s\left(x_{j,k+1}, x_{i\neq j,k}\right) - g_s\left(x_{j,k}, x_{i\neq j,k}\right) \right) \quad \text{(A12)}$$

where the index k refers to one of n subdivisions of the interval between the WW and WS points and the functional notation $g_s(\cdots)$ refers to Eqn A1, evaluated using the arguments given in the parentheses. In Eqn A12, the notation '$x_{i\neq j}$' means 'all variables other than x_j'; thus, the only parameter that differs between the two values of g_s computed in Eqn A12 is x_j. For example, one step in the numerical integration to give p_n would compute the difference in g_s between two adjacent subdivisions (k and $k+1$) using the values of n at k and $k+1$ but using the values at k for all other parameters. The values of each x_j at each index k are defined by supposing that the x_j all change at a uniform pace between the WW and WS conditions. Thus, $x_{j,k} = x_{j,WW} + (k/n) \cdot (x_{j,WS} - x_{j,WW})$. We used $n = 1000$ steps for numerical integration in this study. We then expressed the partial changes as percentages of the value of g_s under WW conditions and defined the resulting percentages as 'contributions' to the total change in g_s between WW and WS conditions:

$$C_j = 100 p_j / g_{s,WW} \quad \text{(A13)}$$

The C_j adds up to the total percent change in g_s. Thus, if g_s declines under WS conditions, the sum of the C_j will be negative, and thus, at least some of the C_j will also be negative.We implemented Eqns A12 and A13 using a Microsoft Excel spreadsheet that carries out the calculations using Visual Basic for Applications (VBA); a spreadsheet containing the VBA code and demonstrating its application to data is included as Supporting File S2.

REFERENCES

Ball J.T., Woodrow I.E. & Berry J.A. (1987) A model predicting stomatal conductance and its contribution to the control of photosynthesis under different environmental conditions. In *Progress in Photosynthesis Research* (ed Biggens J.), pp. 221–224. Martinus-Nijhoff Publishers, Dordrecht, the Netherlands.

Bartlett M.K., Scoffoni C., Ardy R., Zhang Y., Sun S., Cao K. & Sack L. (2012) Rapid determination of comparative drought tolerance traits: using an osmometer to predict turgor loss point. *Methods in Ecology and Evolution* **3**, 880–888.

Bates L.M. & Hall A.E. (1981) Stomatal closure with soil water depletion not associated with changes in bulk leaf water status. *Oecologia* **50**, 62–65.

Bauer H., Ache P., Lautner S., Fromm J., Hartung W., Al-Rasheid K.A.S., … Hedrich R. (2013) The stomatal response to reduced relative humidity requires guard cell-autonomous ABA synthesis. *Current Biology* **23**, 53–57.

Bernacchi C.J., Portis A.R., Nakano H., von Caemmerer S. & Long S.P. (2002) Temperature response of mesophyll conductance. Implications for the determination of RuBisCo enzyme kinetics and for limitations to photosynthesis *in vivo*. *Plant Physiology* **130**, 1992–1998.

Brodribb T.J. & Cochard H. (2009) Hydraulic failure defines the recovery and point of death in water-stressed conifers. *Plant Physiology* **149**, 575–584.

Brodribb T.J. & McAdam S.A.M. (2013) Abscisic acid mediates a divergence in the drought response of two conifers. *Plant Physiology* **162**, 1370–1377.

Buck A.L. (1981) New equations for computing vapor pressure and enhancement factor. *Journal of Applied Meteorology and Climatology* **20**, 1527–1532.

Buckley T.N. & Diaz-Espejo A. (2015) Partitioning changes in photosynthetic rate into contributions from different variables. *Plant, Cell and Environment* **38**, 1200–1211.

Buckley T.N., Martorell S., Diaz-Espejo A., Tomàs M. & Medrano H. (2014) Is stomatal conductance optimized over both time and space in plant crowns? A field test in grapevine (*Vitis vinifera*). *Plant, Cell and Environment* **37**, 2707–2721.

Buckley T.N., Mott K.A. & Farquhar G.D. (2003) A hydromechanical and biochemical model of stomatal conductance. *Plant, Cell and Environment* **26**, 1767–1785.

Buckley T.N. & Mott K.A. (2000) Stomatal responses to non-local changes in PFD: evidence for long-distance hydraulic interactions. *Plant, Cell and Environment* **23**, 301–309.

Buckley T.N. (2005) The control of stomata by water balance. *New Phytologist* **168**, 275–292.

Busch F.A. (2014) Opinion: The red-light response of stomatal movement is sensed by the redox state of the photosynthetic electron transport chain. *Photosynthesis Research* **119**, 131–140.

Choat B., Drayton W.M., Brodersen C., Matthews M.A., Shackel K.A., Wada H. & McElrone A.J. (2010) Measurement of vulnerability to water stress-induced cavitation in grapevine: a comparison of four techniques applied to a long-vesseled species. *Plant, Cell and Environment* **33**, 1502–1512.

Christmann A., Hoffmann T., Teplova I., Grill E. & Mu A. (2005) Generation of active pools of abscisic acid revealed by *in vivo* imaging of water-stressed *Arabidopsis*. *Plant Physiology* **137**, 209–219.

Christmann A., Weiler E.W., Steudle E. & Grill E. (2007) A hydraulic signal in root-to-shoot signalling of water shortage. *The Plant Journal* **52**, 167–174.

Cochard H., Barigah S.T., Kleinhentz M. & Eshel A. (2008) Is xylem cavitation resistance a relevant criterion for screening drought resistance among *Prunus* species? *Journal of Plant Physiology* **165**, 976–982.

Cochard H., Coll L., Le Roux X. & Ameglio T. (2002) Unraveling the effects of plant hydraulics on stomatal closure during water stress in walnut. *Plant Physiology* **128**, 282–290.

Comstock J.P. & Mencuccini M. (1998) Control of stomatal conductance by leaf water potential in *Hymenoclea salsola* (T. & G.), a desert subshrub. *Plant, Cell and Environment* **21**, 1029–1038.

Darwin F. (1898) Observations on stomata. *Philosophical Transactions of the Royal Society of London, Series B* **190**, 531–621.

Davies W.J. & Zhang J. (1991) Root signals and the regulation of growth and development of plants in drying soil. *Annual Review of Plant Physiology and Plant Molecular Biology* **42**, 55–76.

Dewar R.C. (1995) Interpretation of an empirical model for stomatal conductance in terms of guard cell function. *Plant, Cell and Environment* **18**, 365–372.

Dewar R.C. (2002) The Ball–Berry–Leuning and Tardieu–Davies stomatal models: synthesis and extension within a spatially aggregated picture of guard cell function. *Plant, Cell and Environment* **25**, 1383–1398.

Diaz-Espejo A., Buckley T.N., Sperry J.S., Cuevas M.V., de Cires A., Elsayed-Farag S., … Fernández J.E. (2012) Steps toward an improvement in process-based models of water use by fruit trees: a case study in olive. *Agricultural Water Management* **114**, 37–49.

Diaz-Espejo A., Nicolás E. & Fernández J.E. (2007) Seasonal evolution of diffusional limitations and photosynthetic capacity in olive under drought. *Plant, Cell and Environment* **30**, 922–933.

Diaz-Espejo A., Walcroft A.S., Fernández J.E., Hafidi B., Palomo M.J. & Girón I. F. (2006) Modeling photosynthesis in olive leaves under drought conditions. *Tree Physiology* **26**, 1445–1456.

Dodd I.C., Egea G. & Davies W.J. (2008) Abscisic acid signalling when soil moisture is heterogeneous: decreased photoperiod sap flow from drying roots limits abscisic acid export to the shoots. *Plant, Cell and Environment* **31**, 1263–1274.

Dodd I.C. (2005) Root-to-shoot signalling: assessing the roles of 'up' in the up and down world of long-distance signalling *in planta*. *Plant and Soil* **274**, 251–270.
Dodd I.C. (2009) Rhizosphere manipulations to maximize 'crop per drop' during deficit irrigation. *Journal of Experimental Botany* **60**, 2454–2459.
Dodd I.C. (2013) Abscisic acid and stomatal closure: a hydraulic conductance conundrum? *New Phytologist* **197**, 6–8.
Downton W.J.S., Loveys B.R. & Grant W.J.R. (1988) Stomatal closure fully accounts for the inhibition of photosynthesis by abscisic acid. *New Phytologist* **108**, 263–266.
Egea G., González-Real M.M., Baille A., Nortes P.A. & Diaz-Espejo A. (2011) Disentangling the contributions of ontogeny and water stress to photosynthetic limitations in almond trees. *Plant, Cell and Environment* **34**, 962–979.
Egea G., Nortes P.A., González-Real M.M., Baille A. & Domingo R. (2010) Agronomic response and water productivity of almond trees under contrasted deficit irrigation regimes. *Agricultural Water Management* **97**, 171–181.
Ethier G.J. & Livingston N.J. (2004) On the need to incorporate sensitivity to CO_2 transfer conductance into the Farquhar–von Caemmerer–Berry leaf photosynthesis model. *Plant, Cell and Environment* **27**, 137–153.
Farquhar G.D., von Caemmerer S. & Berry J.A. (1980) A biochemical model of photosynthetic CO_2 assimilation in leaves of C_3 species. *Planta* **149**, 78–90.
Farquhar G.D. & Wong S.C. (1984) An empirical model of stomatal conductance. *Australian Journal of Plant Physiology* **11**, 191–209.
Fernández J.E., Rodriguez-Dominguez C.M., Perez-Martin A., Zimmermann U., Rüger S., Martín-Palomo M.J., … Diaz-Espejo A. (2011) Online-monitoring of tree water stress in a hedgerow olive orchard using the leaf patch clamp pressure probe. *Agricultural Water Management* **100**, 25–35.
Fernández J.E., Perez-Martin A., Torres-Ruiz J.M., Cuevas M.V., Rodriguez-Dominguez C.M., Elsayed-Farag S., … Diaz-Espejo A. (2013) A regulated deficit irrigation strategy for hedgerow olive orchards with high plant density. *Plant and Soil* **372**, 279–295.
Flexas J., Bota J., Loreto F., Cornic G. & Sharkey T.D. (2004) Diffusive and metabolic limitations to photosynthesis under drought and salinity in C3 plants. *Plant Biology* **6**, 269–279.
Franks P.J., Buckley T.N., Shope J.C. & Mott K.A. (2001) Guard cell volume and pressure measured concurrently by confocal microscopy and the cell pressure probe. *Plant Physiology* **125**, 1577–1584.
Franks P.J. & Farquhar G.D. (2007) The mechanical diversity of stomata and its significance in gas-exchange control. *Plant Physiology* **143**, 78–87.
Franks P.J. (2013) Passive and active stomatal control: either or both? *New Phytologist* **198**, 325–327.
Fuchs E.E. & Livingston N.J. (1996) Hydraulic control of stomatal conductance in Douglas fir [*Pseudotsuga menziesii* (Mirb) Franco] and alder [*Alnus rubra* (Bong)] seedlings. *Plant, Cell and Environment* **19**, 1091–1098.
Goodger J.Q.D. & Schachtman D.P. (2010) Re-examining the role of ABA as the primary long-distance signal produced by water-stressed roots. *Plant Signaling and Behavior* **5**, 1298–1301.
Grantz D.A. & Zeiger E. (1986) Stomatal responses to light and leaf–air water vapor pressure difference show similar kinetics in sugarcane and soybean. *Plant Physiology* **81**, 865–868.
Hetherington A.M. & Woodward F.I. (2003) The role of stomata in sensing and driving environmental change. *Nature* **424**, 901–908.
Hetherington A.M. (2001) Guard cell signaling. *Cell* **107**, 711–714.
Hinckley T.M., Duhme F., Hinckley A.R. & Richter H. (1980) Water relations of drought hardy shrubs: osmotic potential and stomatal reactivity. *Plant, Cell and Environment* **3**, 131–140.
Holbrook N.M., Shashidhar V.R., James R.A. & Munns R. (2002) Stomatal control in tomato with ABA-deficient roots: response of grafted plants to soil drying. *Journal of Experimental Botany* **53**, 1503–1514.
Huber K., Vanderborght J., Javaux M., Schröder N., Dodd I.C. & Vereecken H. (2014) Modelling the impact of heterogeneous rootzone water distribution on the regulation of transpiration by hormone transport and/or hydraulic pressures. *Plant and Soil* **384**, 93–112.
Iwanoff L. (1928) Zur Methodik der Transpirations-bestimmung am Standort. *Berichte. Deutsche Botanische Gesellschaft* **46**, 306–310.
Jarvis P.G. (1976) The interpretation of the variations in leaf water potential and stomatal conductance found in canopies in the field. *Philosophical Transactions of the Royal Society of London, Series B* **273**, 593–610.
Lawson T., Simkin A.J., Kelly G. & Granot D. (2014) Mesophyll photosynthesis and guard cell metabolism impacts on stomatal behaviour. *New Phytologist* **203**, 1064–1081.
Li B., Feng Z., Xie M., Sun M., Zhao Y., Liang L., … Jia W. (2011) Modulation of the root-sourced ABA signal along its way to the shoot in *Vitis riparia* x *Vitis labrusca* under water deficit. *Journal of Experimental Botany* **62**, 1731–1741.
Manzi M., Lado J., Rodrigo M.J., Zacarías L., Arbona V. & Gómez-Cadenas A. (2015) Root ABA accumulation in long-term water-stressed plants is sustained by hormone transport from aerial organs. *Plant and Cell Physiology* **56**, 2457–2466.
Martorell S., Medrano H., Tomàs M., Escalona J.M., Flexas J. & Diaz-Espejo A. (2015) Plasticity of vulnerability to leaf hydraulic dysfunction during acclimation to drought in grapevines: an osmotic-mediated process. *Physiologia Plantarum* **153**, 381–391.
McAdam S.A.M., Sussmilch F.C. & Brodribb T.J. (2016) Stomatal responses to vapour pressure deficit are regulated by high speed gene expression in angiosperms. *Plant, Cell and Environment* **39**, 485–491.
Meidner H. (1986) Cuticular conductance and the humidity response of stomata. *Journal of Experimental Botany* **37**, 517–525.
Monteith J.L. (1995) A reinterpretation of stomatal responses to humidity. *Plant, Cell and Environment* **18**, 357–364.
Mott K.A. & Franks P.J. (2001) The role of epidermal turgor in stomatal interactions following a local perturbation in humidity. *Plant, Cell and Environment* **24**, 657–662.
Mott K.A. & Parkhurst D.F. (1991) Stomatal responses to humidity in air and helox. *Plant, Cell and Environment* **14**, 509–515.
Mott K.A. (1988) Do stomata respond to CO_2 concentrations other than intercellular? *Plant Physiology* **86**, 200–203.
Mott K.A. (2009) Opinion: stomatal responses to light and CO_2 depend on the mesophyll. *Plant, Cell and Environment* **32**, 1479–1486.
Munemasa S., Hauser F., Park J., Waadt R., Brandt B. & Schroeder J.I. (2015) Mechanisms of abscisic acid-mediated control of stomatal aperture. *Current Opinion in Plant Biology* **28**, 154–162.
Pantin F., Monnet F., Jannaud D., Costa J.M., Renaud J., Muller B. & Genty B. (2012) The dual effect of abscisic acid on stomata. *New Phytologist* **197**, 65–72.
Passioura J.B. (2006) The perils of pot experiments. *Functional Plant Biology* **33**, 1075–1079.
Peak D. & Mott K.A. (2011) A new, vapour-phase mechanism for stomatal responses to humidity and temperature. *Plant, Cell and Environment* **34**, 162–178.
Perez-Perez J.G., Dodd I.C. & Botia P. (2012) Partial rootzone drying increases water-use efficiency of lemon Fino 49 trees independently of root-to-shoot ABA signaling. *Functional Plant Biology* **39**, 366–378.
Perks M.P., Irvine J. & Grace J. (2002) Canopy stomatal conductance and xylem sap abscisic acid (ABA) in mature Scots pine during a gradually imposed drought. *Tree Physiology* **22**, 877–883.
Premachandra G.S., Saneoka H., Fujita K. & Ogata S. (1992) Osmotic adjustment and stomatal response to water deficits in maize. *Journal of Experimental Botany* **43**, 1451–1456.
R Core Team. (2014) R: a language and environment for statistical computing. R Foundation for Statistical Computing, Vienna, Austria. URL http://www.R-project.org/.
Raschke K. (1970) Stomatal responses to pressure changes and interruptions in the water supply of detached leaves of *Zea mays* L. *Plant Physiology* **45**, 415–423.
Romero P., Dodd I.C. & Martinez-Cutillas A. (2012) Contrasting physiological effects of partial root zone drying in field-grown grapevine (*Vitis vinifera* L. cv. Monastrell) according to total soil water availability. *Journal of Experimental Botany* **63**, 4071–4083.
Rufelt H. (1963) Rapid changes in transpiration in plants. *Nature* **197**, 985–986.
Sack L., Pasquet-Kok J. & PrometheusWiki contributors. (2011) Leaf pressure–volume curve parameters. URL http://prometheuswiki.publish.csiro.au/tiki-index.php?page=Leaf+pressure-volume+curve+parameters [accessed 9 October 2014].
Sadras V.O. (2009) Does partial root-zone drying improve irrigation water productivity in the field? A meta-analysis. *Irrigation Science* **27**, 183–190.
Schachtman D.P. & Goodger J.Q.D. (2008) Chemical root to shoot signaling under drought. *Trends in Plant Science* **13**, 281–287.
Secchi F., Perrone I., Chitarra W., Zwieniecka A., Lovisolo C. & Zwieniecki M. (2013) The dynamics of embolism refilling in abscisic acid (ABA)-deficient tomato plants. *International Journal of Molecular Sciences* **14**, 359–377.
Shangguan Z., Shao M. & Dyckmans J. (1999) Interaction of osmotic adjustment and photosynthesis in winter wheat under soil drought. *Journal of Plant Physiology* **154**, 753–758.
Sperry J.S., Hacke U.G., Oren R. & Comstock J.P. (2002) Water deficit and hydraulic limits to leaf water supply. *Plant, Cell and Environment* **25**, 251–263.
Sperry J.S. (2000) Hydraulic constraints on gas exchange. *Agricultural and Forest Meteorology* **104**, 13–23.
Tardieu F. & Davies W.J. (1992) Stomatal response to abscisic acid is a function of current plant water status. *Plant Physiology* **98**, 540–545.

Tardieu F. & Davies W.J. (1993) Integration of hydraulic and chemical signalling in the control of stomatal conductance and water status of droughted plants. *Plant, Cell and Environment* **16**, 341–349.

Tardieu F., Simmoneau T. & Parent B. (2015) Modelling the coordination of the controls of stomatal aperture, transpiration, leaf growth, and abscisic acid: update and extension of the Tardieu–Davies model. *Journal of Experimental Botany* **66**, 2227–2237.

Tardieu F. & Simonneau T. (1998) Variability among species of stomatal control under fluctuating soil water status and evaporative demand: modelling isohydric and anisohydric behaviours. *Journal of Experimental Botany* **49**, 419–432.

Tardieu F. (1993) Will increases in our understanding of soil–root relations and root signalling substantially alter water flux models? *Philosophical Transactions of the Royal Society of London B* **341**, 57–66.

Torres-Ruiz J.M., Diaz-Espejo A., Perez-Martin A. & Hernandez-Santana V. (2015) Role of hydraulic and chemical signals in leaves, stems and roots in the stomatal behaviour of olive trees under water stress and recovery conditions. *Tree Physiology* **35**, 415–424.

Turner N., Begg J. & Tonnet M. (1978) Osmotic adjustment of sorghum and sunflower crops in response to water deficits and its influence on the water potential at which stomata close. *Australian Journal of Plant Physiology* **5**, 597–608.

USDA (2010) *Keys to Soil Taxonomy*11th edn, pp. 334. United States Department of Agriculture, Natural Resource Conservation Service, Washington, DC, USA.

Waadt R., Hitomi K., Nishimura N., Hitomi C., Adams S.R., Getzoff E.D. & Schroeder J.I. (2014) FRET-based reporters for the direct visualization of abscisic acid concentration changes and distribution in Arabidopsis. *eLife* **3**, 1–28.

Whitehead D., Livingston N.J., Kelliher F.M., Hogan K.P., Pepin S., McSeveny T. M. & Byers J.N. (1996) Response of transpiration and photosynthesis to a transient change in illuminated foliage area for a *Pinus radiata* D. Don tree. *Plant, Cell and Environment* **19**, 949–957.

Yao C., Moreshet S. & Aloni B. (2001) Water relations and hydraulic control of stomatal behaviour in bell pepper plant in partial soil drying. *Plant, Cell and Environment* **24**, 227–235.

Received 22 February 2016; received in revised form 17 May 2016; accepted for publication 17 May 2016

SUPPORTING INFORMATION

Additional Supporting Information may be found in the online version of this article at the publisher's web-site:

Table S1. Parameter values used in this study for responses of photosynthetic parameters to temperature. Values at 25 °C (y_{25}) varied across leaves, treatments and species, except that we assumed $y_{25} = 272.38$ Pa for K_c, 165.82 kPa for K_o and 37.43 Pa for Γ_*, based on Bernacchi *et al*. (2002). $T_r = 298.15$ K.

Table S2. Photosynthetic parameter values measured in this study. Values at 25 °C are shown. Asterisks denote significant treatment effects within species: *, $P < 0.05$; **, $P < 0.01$.

Figure S1. Measurements of stomatal conductance in relation to PPFD in (a) almond, (b) olive and (c) grapevine. In (a), measurements were made under similar Δw; in (b), Δw varied between 14.4 and 38.3 mmol mol^{-1}, and in (c), Δw varied between 3.4 and 18.2 mmol mol^{-1}. These data are shown to validate the assumption that the response of g_s to PPFD is approximately homogeneous (i.e. g_s approaches zero at zero PPFD) in almond and olive, and in grapevine in the WS treatment. The response is not homogeneous for grapevine in WW; however, the lowest range of PPFD shown here ($<50\ \mu$mol m^{-2} s^{-1}) only occurred at the latest measurement time in the diurnal cycle (8 PM), at which time PPFD was rapidly declining and g_s was likely not at steady state.

Figure S2. Relationship between measured stomatal conductance, g_s, and calculated leaf turgor, P (midday averages, between 1100 and 1400 h Greenwich Mean Time [GMT]), under well-watered (WW, closed symbols) and water-stressed (WS, open symbols) conditions in almond (circles), grapevine (triangles) and olive (squares). Error bars are SEs ($n = 6$ to 10).

Figure S3. Relationship between measured and fitted values of soil-to-leaf hydraulic conductance, K (slope = 0.87, $r^2 = 0.69$, $P < 0.0001$) of almond (circles), grapevine (triangles) and olive (squares) under well-watered (closed symbols) and water-stressed (open symbols) conditions. Measured K was estimated as $g_s\Delta w/(\Psi_{soil} - \Psi_{leaf})$ and data shown are midday averages (between 1100 and 1400 h GMT). Fitted K was estimated by fitting Eqn 5 to diurnal measurements of stomatal conductance, g_s, in four (almond and olive) and five (grapevine) different leaves, using Solver in Microsoft Excel to minimize the sum of squared differences between modelled and measured g_s. The turgor-independent parameter n was also estimated but data are not shown. Bars are standard errors: $n = 4$ (almond and olive) and $n = 5$ (grapevine).